bad (in the sense of having a bottomless spectrum) already in the two-body problem. This known defect (pointed out by G. Breit) can be reparied without upsetting the fit to the two-body scattering data, but the resulting potential [T. Hamada, Y. Nakamura, and R. Tamagaki, Progr. Theor. Phys. 33, 769 (1965)] continues to be bad for the many-body problem.

[5]E. Rochleder and K. Erkelenz, Phys. Rev. 172, 1013 (1968); C. N. Bressel, A. K. Kerman, and B. Rouben, Nucl. Phys. A124, 624 (1969).

[6]K. E. Lassila, M. H. Hull, Jr., H. M. Ruppel, F. A. McDonald, and G. Breit, Phys. Rev. 126, 881 (1962).

[7]R. Tamagaki, Progr. Theor. Phys. 39, 91 (1968).

[8]D. Kiang, M. A. Preston, and P. Yip, Phys. Rev. 170, 907 (1968). The bottomlessness of the energy spectrum associated with this potential is apparent by inspection, due to the presence of a term of type $p^2\vec{L}\cdot\vec{S}$ that is cubic in the momentum and can contribute with either sign. The associated singularity in the radial Schrödinger equation for two-body scattering in the triplet state was noticed by these authors; its relevance to the energy spectrum was not discussed.

[9]F. Calogero and Yu. A. Simonov, to be published.

[10]F. Calogero and Yu. A. Simonov, to be published.

ELECTROMAGNETIC STRUCTURE OF THE He^3 NUCLEUS*

J. S. McCarthy, I. Sick,† R. R. Whitney, and M. R. Yearian
High Energy Physics Laboratory and Department of Physics, Stanford University, Stanford, California 94305
(Received 24 July 1970)

The electromagnetic structure of the He^3 nucleus has been investigated by means of high-energy electron scattering. A separation of the charge and magnetic form factors has been accomplished. The charge form-factor data extend to $q^2=20\ \mathrm{fm}^{-2}$ and exhibit a diffraction minimum at $q^2=11.6\ \mathrm{fm}^{-2}$; the magnetic scattering is measured to $q^2=12.5\ \mathrm{fm}^{-2}$. The results are discussed in terms of models for the charge and magnetic distributions of the nucleus.

Among the techniques employed in the investigation of the electromagnetic structure of nuclei, high-energy electron scattering remains extremely useful. By using electrons as the nuclear probe it is possible to separate the scattering mechanism from the nuclear properties one wishes to measure. We have taken measurements on He^3 because of the importance of the three-body problem in strong-interaction theory.

The primary starting point in the description of the scattering process is the one-photon exchange approximation. It is necessary to make some further assumptions before applying the general result to the He^3 nucleus. The first-order correction to the plane-wave Born approximation due to Coulomb distortion is included by using a corrected four-momentum transfer, $q_{\mathrm{eff}}=q(1+\frac{4}{3}Z\alpha/pr_{\mathrm{rms}})$, in the analysis; this result is expected to be quite accurate for the low-Z nucleus He^3.[1] The effects due to intermediate excitation of the nucleus (dispersion corrections) are ignored. Again these corrections are expected to be small for He^3 and will not change the final result.[2-4]

The kinematic effects of the nuclear recoil were included; however, they were neglected in the nuclear matrix elements. Previous estimates of the error incurred in this approximation were of the order q/M.[5,6] More recent calculations on the difference between the relativistic form factor and its nonrelativistic limit have estimated that for the He^3 nucleus and the large momentum transfer considered here, the correction can be on the order of 10%.[7] In this preliminary analysis we neglected the nuclear recoil in the Born-approximation matrix element and in the same spirit performed the partial-wave phase-shift calculation in the center-of-mass frame.

In Born approximation the differential scattering cross section from the spin-$\frac{1}{2}$ He^3 nucleus, with anomalous magnetic moment K, charge Ze, and mass M, can be represented as follows (where $\hbar=c=1$):

$$\frac{d\sigma}{d\Omega}=\left(\frac{Z\alpha}{2E}\right)^2\frac{\cos^2(\theta/2)}{\sin^4(\theta/2)[1+(2E/M)\sin^2(\theta/2)]}\times\left(\frac{F_{\mathrm{ch}}^2(q^2)+F_{\mathrm{mag}}^2(q^2)(1+K)^2(q^2/4M^2)[1+2(1+q^2/4M^2)\tan^2(\theta/2)]}{(1+q^2/4M^2)}\right). \quad (1)$$

The two form factors F_{ch} and F_{mag} are identified with the Fourier transforms of the spatial distribution of the charge and magnetic moment:

$$F_{ch}(q^2)=\frac{4\pi}{Zq}\int_0^\infty \rho(r)\sin(qr)rdr, \tag{2}$$

where

$$F_{ch}(0)=1, \quad \rho(r)=\frac{Z}{2\pi^2}\int_0^\infty \frac{q}{r}\sin(qr)F_{ch}(q^2)dq,$$

and similar equations for F_{mag}.

The interpretation of the magnetic form factor is made more difficult by the existence of magnetic exchange effects. However, exchange contributions to the charge form factor are quite small and therefore these data provide the most accurate source of information on the He^3 ground-state wave function. Previous data[8] on the form factors for He^3 extended to $q^2=8$ fm^{-2} and were characterized by very little structure. It was possible to explain the data with wave functions that were inconsistent with other experimental results (see Delves and Phillips[9] for a review of these calculations). The earlier elastic data represented primarily a determination of the root mean square radius r_{rms}. In order to investigate the He^3 wave function at small distances it was necessary to increase the momentum transfer significantly.

The beam of high-energy electrons was supplied by the Stanford Mark III linear accelerator. A detailed description of the associated experimental equiment can be found in Sick and McCarthy.[10] The system consists primarily of the following: (1) the control of beam resolution, energy (±0.1%), and position (±0.5 mm); (2) the 183-cm double-focusing momentum-analyzing spectrometer; (3) a 100-channel coincidence detector; and (4) an on-line computer analysis.

The essential feature of this experiment consisted of a liquid He^3 and He^4 target contained in a cryogenic Dewar.[11] The target thickness and energy resolution attainable with a liquid target made it possible to perform the described experiment at the high values of q. The He^3 target had an average thickness of 100 mg/cm^2 and was enclosed within thin aluminum windows. The condensed liquid He^3 was held at a temperature of approximately 1.8°K by pumping on the refrigerating liquid He^4. The He^3 target was then pressurized to approximately 300 Torr to operate off the saturated vapor pressure curve, thereby reducing the possibility of local bubbling due to the intense electron beam. A detailed description of the liquid target Dewar and its operation will be published elsewhere.

During the experimental runs, cross sections were simultaneoulsy measured for He^3, He^4, and the aluminum background. Average beam currents of up to 1.5 μA were used with no local bubbling observed in the liquid He^3 although density corrections (~8%) were made because of uniform temperature changes in the liquid. The absolute system efficiency was measured by taking elastic-proton cross sections at the same experimental conditions. The stability and relative normalization during the course of the experiment was determined by the scattering from the extremely stable superfluid He^4. The experimental data were corrected for the relative efficiencies of the individual counters and the important radiation effects—Schwinger and target bremsstrahlung.

The separation of the charge and magnetic form factor was accomplished by using Rosenbluth plots as a function of the effective q. The magnetic-moment distribution was then obtained using the Fourier transform of F_{mag}. The Born approximation was also used for analysis with a preliminary charge distribution; however, the final result was obtained by solving for the phase shift of each partial wave associated with a Dirac electron scattered by a phenomenological central charge density.[12] The charge form factor calculated using the same density is identical within our statistical errors for both methods if the corrected four-momentum q_{eff} is used. The basic distribution used to fit the charge (magnetic) scattering is

$$\rho(r)=Z\left[\frac{\exp(-r^2/4a^2)}{8\pi^{3/2}a^3}-\left(\frac{b^2}{2\pi^{3/2}}\right)\left(\frac{6c^2-r^2}{16c^7}\right)\exp\left(\frac{-r^2}{4c^2}\right)\right], \tag{3}$$

where, in Born approximation,

$$F_B(q^2)=e^{-a^2q^2}-b^2q^2e^{-c^2q^2}. \tag{4}$$

This distribution gives an excellent fit to the charge form factor out to $q^2 = 8\ \mathrm{fm}^{-2}$ and to the magnetic data to the maximum measured value at $q^2 = 12.5\ \mathrm{fm}^{-2}$. To produce the diffraction minimum in the He^3 charge form factor, it was necessary to add a modification $\Delta\rho(r)$ to the charge density:

$$\Delta\rho(r) = \frac{Zdpq_0^2}{2\pi^{3/2}}\left[\frac{\sin(q_0 r)}{q_0 r} + \frac{p^2}{2q_0^2}\cos(q_0 r)\right]\exp(-\tfrac{1}{4}p^2r^2), \qquad (5)$$

$$\Delta F_B(q^2) = d\exp\left[-\left(\frac{q-q_0}{p}\right)^2\right]. \qquad (6)$$

The free parameters are a, b, c, d, p, and q_0. The observed diffraction minimum is at $q^2 = 11.6\ \mathrm{fm}^{-2}$.

A Rosenbluth plot taken at $q^2 = 14\ \mathrm{fm}^{-2}$ did not show any detectable magnetic-scattering contribution and the possible modification of the magnetic density at small radii awaits further experimental evidence. The charge form factor for He^3 together with the best fit for $\rho(r) + \Delta\rho(r)$ is shown in Fig. 1; the data for the magnetic moment are shown in Fig. 2. The errors quoted include counting statistics and the possibility of a ±3% absolute normalization error.

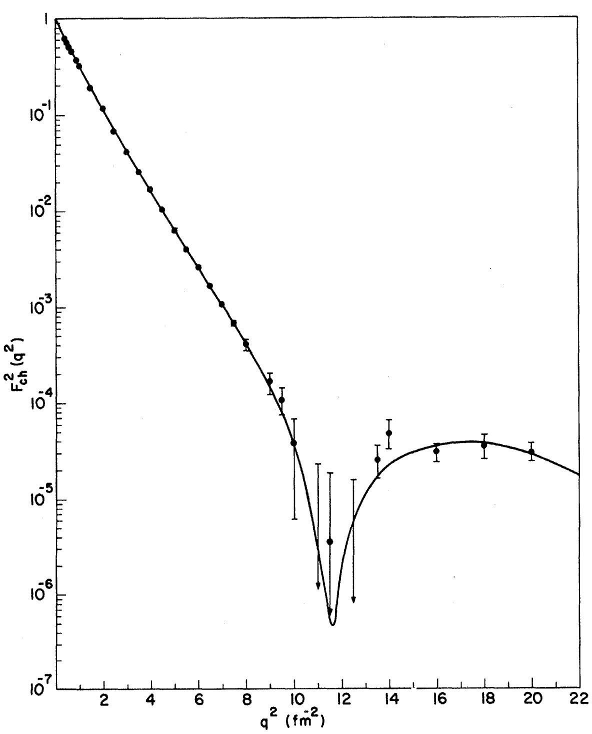

FIG. 1. He^3 charge form factor. The best fit to the data has the following parameters for $\chi^2 = 0.7$ per degree of freedom: $a = 0.675 \pm 0.008$ fm; $b = 0.366 \pm 0.025$ fm; $c = 0.836 \pm 0.032$ fm; $d = (-6.78 \pm 0.83) \times 10^{-3}$; $q_0 = 3.98 \pm 0.09\ \mathrm{fm}^{-1}$; $p = 0.90 \pm 0.16\ \mathrm{fm}^{-1}$. The value of r_{rms}^c for this fit is 1.88 ± 0.05 fm. The form factors calculated from the phase shift program have been folded with the experimental angular resolution of $\Delta\theta = \pm 0.93°$.

The charge radius value of $r_{\mathrm{rms}}^c = 1.88 \pm 0.05$ fm is in agreement with Ref. 8 (1.87 ± 0.05 fm); the magnetic value of $r_{\mathrm{rms}}^m = 1.95 \pm 0.11$ fm is in agreement with the recent 180° scattering measurements,[13] $r_{\mathrm{rms}}^m = 1.94$ fm, but in disagreement with Ref. 8 (1.74 ± 0.10 fm). A Fermi distribution will give a good fit to the charge data only up to $q^2 \approx 7\ \mathrm{fm}^{-2}$, with an $r_{\mathrm{rms}}^c = 1.90$ fm. The fact that the magnetic radius is larger than the charge radius is in contradiction to the earlier results, and tends to disprove the simple assumption that the opposite case should be true because of the greater binding of the neutron through the triplet interaction. The present data should provide accurate estimates of the dominant contributions to the ground-state nuclear wave functions in terms of S, S', P, and D states,[14,15]

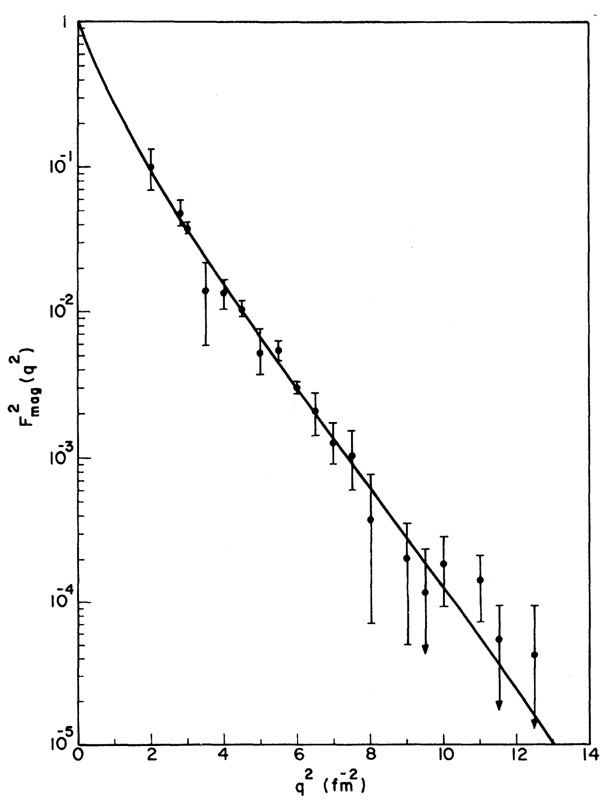

FIG. 2. He^3 magnetic form factor and the best-fit parameter values for $\chi^2 = 0.9$ per degree of freedom: $a = 0.654 \pm 0.024$ fm; $b = 0.456 \pm 0.029$ fm; $c = 0.821 \pm 0.053$ fm. The magnetic radius is $r_{\mathrm{rms}}^m = 1.95 \pm 0.11$ fm.

as well as for the q^2 dependence of the magnetic exchange form factor.

The He^3 charge distribution as determined from the data is shown in Fig. 3. The noticeable curvature in F_{ch} in the region $q^2=0$ to $6\ fm^{-2}$ is well represented by the significant tail in the charge distribution at large radii. The central depression of approximately 15% is required by the presence of the diffraction minimum. The difference in the charge radii for He^3 and He^4 ($r_{rms}=1.71$ fm) can be understood in terms of the independent-particle shell model using a finite potential well. We have calculated the shell-model wave functions using a Woods-Saxon well and fitting the known proton separation energies. With the assumption of an "equivalent" Gaussian core of radius = 1.68 fm in the local potential, the effect of a finite well is to add 0.04 fm and 0.21 fm to the rms radii of He^4 and He^3, respectively. In this simple approximation the increase (of 0.17 fm) in the He^3 charge radius over that for He^4 can be primarily understood in terms of the reduced binding energy; the inadequacy of using Gaussian wave functions for He^3 is clearly shown.

At the values of the momentum transfer reached in this experiment, the details of the structure of

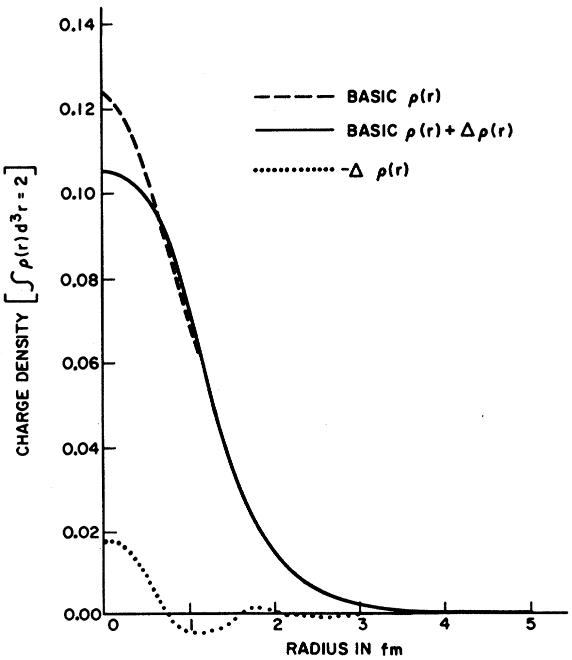

FIG. 3. He^3 charge distribution; basic $\rho(r)$ represents the distribution given by Eq. (3), the modification added is $\Delta\rho(r)$ from Eq. (5). These distributions are shown for the best-fit parameters in the caption for Fig. 1.

the wave function at radii less than 1 fm are evident. It is possible that the elastic form factors may now provide an important source of information concerning the basic nucleon-nucleon interaction. In particular the measured center distributions are sensitive to, and may discriminate between, the two basic models for the short-range interaction[16]: a hole in the wave function extending to approximately 0.5 fm in radius as suggested by vector-meson repulsion,[17] or extending to 0.7 fm as implied by the boundary-condition model.[18]

While it is true that the case for some type of short-range repulsion is strengthened by these new data, the method of considering these nucleon-nucleon interactions in the three-body problem requires a more detailed analysis than has previously been attempted for electron scattering results.

It is difficult to judge the relevancy of including phenomenological "soft" or "hard" cores while at the same time using unrealistic two-nucleon potentials. This is certainly the case for a model using a Gaussian basis, since the central "cores" then introduced just tend to mask the physical unreality of the initial assumption. Certainly a better but more difficult approach would be to start with a potential that agrees with the experimental two-nucleon data and then use this in a realistic three-body calculation.

The comparison with other experimental information is important from this standpoint. For example, if the nucleon-nucleon strong interaction is charge symmetric and if no charge-asymmetric three-body force exists, then the difference in binding energy between He^3 and H^3 must be attributed to electromagnetic effects. Detailed calculations of this difference using previous values for the form factors have tended to be approximately 0.1 MeV too low[19]; the new data represent a more diffuse electromagnetic structure for He^3 and therefore would tend to increase this disagreement.

We wish to acknowledge the support of Professor Robert Hofstadter during the course of this experiment. One of us (J.S.M.) is grateful for the many discussions with Dr. Reinhard Frosch which motivated the present experiment.

---

*Work supported in part by the National Science Foundation and the Office of Naval Research under Contract No. 225(67).

†Present address: Centre d'Etudes Nucléaires de Saclay, B. P. No. 2, 94 Gif-Sur-Yvette, France.

[1]T. DeForest, Jr., and J. D. Walecka, Advan. Phys. 15, 1 (1966).
[2]C. Toepffer and D. Drechsel, Phys. Rev. Lett. 24, 1131 (1970).
[3]D. S. Onley, Nucl. Phys. A118, 436 (1968).
[4]G. H. Rawitscher, Phys. Rev. 151, 846 (1966).
[5]L. L. Foldy, K. W. Ford, and D. R. Yennie, Phys. Rev. 113, 1147 (1959).
[6]G. B. West, Phys. Rev. 139, B1246 (1965).
[7]G. Cocho and J. Flores, Nucl. Phys. A143, 529 (1970), and Phys. Lett. 31B, 639 (1970).
[8]H. Collard, R. Hofstadter, E. B. Hughes, A. Johansson, M. R. Yearian, R. B. Day, and R. T. Wagner, Phys. Rev. 138, B57 (1965).
[9]L. M. Delves and A. C. Phillips, Rev. Mod. Phys. 41, 497 (1969).
[10]I. Sick and J. S. McCarthy, to be published.
[11]The external Dewar was supplied by Cryogenic Associates, Indianapolis, Ind.
[12]J. Heisenberg, private communication.
[13]B. T. Chertok, E. C. Jones, W. L. Bendel, and L. W. Fagg, Phys. Rev. Lett. 23, 34 (1969).
[14]L. I. Schiff, Phys. Rev. 133, B802 (1964).
[15]B. F. Gibson and L. I. Schiff, Phys. Rev. 138, B26 (1965).
[16]This possibility was suggested by Professor H. P. Noyes.
[17]R. V. Reid, Jr., Ann. Phys. 50, 411 (1968).
[18]E. L. Lomon and H. Feshbach, Rev. Mod. Phys. 39, 611 (1967).
[19]K. Okamoto and C. Lucas, Nucl. Phys. B2, 347 (1967).

ISOBARIC ANALOG RESONANCE WIDTHS AND THE DISTRIBUTION OF COULOMB MIXING STRENGTH IN NUCLEI

A. Z. Mekjian*
Department of Physics, Rutgers, The State University, New Brunswick, New Jersey 08903
(Received 13 July 1970)

Experimental data on the microgiant spreading widths of analog resonances indicate that these widths decrease slightly with increasing mass number A for $A=37$-50 and then increase again for $A>60$. A calculation is presented in which this remarkable property can be understood in terms of a model in which the distribution of Coulomb mixing strength in a nucleus has two peaks with the analog state lying between these two peaks and moving with respect to them with changes in A and T_ζ.

With the increasing number of analog-state resonance experiments, systematic trends of various properties associated with these resonances have emerged. Specifically, the spreading widths of analog-state resonances have been extracted fairly accurately for a number of nuclei (see Table I). An interesting experimental feature of these widths is that they have a minimal value as a function of A for nuclei with $A \approx 50$. The significance of this remarkable feature has motivated this Letter. In particular, we report on a calculation which predicts a minimum in this width at the experimentally observed value.

The spreading width of an analog state describes its average decay into the dense spectrum of normal (T-lower) isospin states which surround it, and therefore proceeds through charge-dependent forces. In the presence of such forces the strength of the analog state, measured, for example, by its proton-emission width, will be shared among nearby levels of the compound nuclear system. Moreover, the averaged proton strength distribution has a single peak of a near Lorentzian shape, with a width given by

$$\Gamma_a^{\downarrow} = 2\pi\langle |V|^2\rangle \rho(E_a). \tag{1}$$

Here, $\langle |V|^2\rangle$ denotes the mean square isospin-nonconserving matrix element between the analog state $\psi_a(T=T_\zeta, T_\zeta-1)$ and the T-lower states $\psi_\lambda(T=T_\zeta-1, T_\zeta-1)$, while $\rho(E_a)$ represents the density of these latter states at the analog energy E_a.

To obtain $\Gamma_a^{\downarrow}$, we first calculate the sum of the squares of the transition-matrix elements[1] from the analog to all normal isospin states ψ_λ. We restrict ourselves, for the moment, to the isovector part C_V of the Coulomb force and write for this strength the expression

$$M_V(T_\zeta-1) = \textstyle\sum_\lambda |\langle\psi_a|C_V|\psi_\lambda\rangle|^2.$$

This expression can then be simplified (by use of closure) to

$$M_V(T_\zeta-1) = \langle\psi_a|C_V P_{T_\zeta-1} C_V|\psi_a\rangle,$$

where $P_{T_\zeta-1}$ projects onto states with $T=T_\zeta-1$. Then, using uncorrelated statistical-model wave functions in which the density $\rho(r)$ of each nucleon